ACS APPLIED MATERIALS & INTERFACES

Research Article

www.acsami.org

Micropatterning Extracellular Matrix Proteins on Electrospun Fibrous Substrate Promote Human Mesenchymal Stem Cell Differentiation Toward Neurogenic Lineage

Huaqiong Li,[*,†,‡,§] Feng Wen,[§] Huizhi Chen,[§] Mintu Pal,[§] Yuekun Lai,[▽] Allan Zijian Zhao,[‡] and Lay Poh Tan[*,§]

[†]Institute of Biomaterials and Engineering, Wenzhou Medical University, Chashan Higher Education Zone, Wenzhou 325035, China

[‡]Wenzhou Institute of Biomaterials and Engineering, Chinese Academy of Sciences, 16 Xinsan Road, Wenzhou 325011, China

[§]School of Materials Science and Engineering, Nanyang Technological University, 50 Nanyang Avenue, 639798, Singapore

[▽]National Engineering Laboratory of Modern Silk, College of Textile and Clothing Engineering, Soochow University, Suzhou 215123, China

Supporting Information

ABSTRACT: In this study, hybrid micropatterned grafts constructed via a combination of microcontact printing and electrospinning techniques process were utilized to investigate the influencing of patterning directions on human mesenchymal stem cells (hMSCs) differentiation to desired phenotypes. We found that the stem cells could align and elongate along the direction of the micropattern, where they randomly distributed on nonmicropatterned surfaces. Concomitant with patterning effect of component on stem cell alignment, a commensurate increase on the expression of neural lineage commitment markers, such as microtubule associated protein 2 (MAP2), Nestin, NeuroD1, and Class III β-Tubulin, were revealed from mRNA expression by quantitative Real Time PCR (qRT-PCR) and MAP2 expression by immunostaining. In addition, the effect of electrospun fiber orientation on cell behaviors was further examined. An angle of 45° between the direction of micropatterning and orientation of aligned fibers was verified to greatly prompt the outgrowth of filopodia and neurogenesis of hMSCs. This study demonstrates that the significance of hybrid components and electrospun fiber alignment in modulating cellular behavior and neurogenic lineage commitment of hMSCs, suggesting promising application of porous scaffolds with smart component and topography engineering in clinical regenerative medicine.

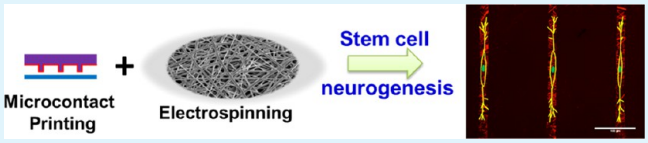

KEYWORDS: *microcontact printing, electrospinning, biomaterials, stem cell, neurogenesis*

INTRODUCTION

Control of stem cell fate using various biochemical and physical cues incorporated onto the scaffold is a critical challenge to achieve goals in biomedical applications. The scaffold, which is normally a highly porous substrate, provides a biomolecular, structural, and mechanical interface on which cells survive, functionalize and generate new extracellular matrix (ECM, including proteins and saccharides) that makes up living tissue.[1] While much effect has been dedicated to utilize soluble biochemical factors (e.g., growth factors, chemicals, hormones, etc.) to direct stem cell proliferation and differentiation, investigators have recently begun to acknowledge the effect of physical factors on cell behavior. The physical cues may comprise applied mechanical stress/tension, electric field, magnetic field, and/or topography.[2−5] Interestingly, regardless of the type of physical stimuli applied, changes in cellular morphology almost always to be the first to be observed.[6−8] Biophysical stimuli of ECM stimulate cells through the activation of focal adhesion kinase and reorganization of cytoskeletons.[9−11] This results in the induction of signaling cascades that affect cell growth, such as cell proliferation and differentiation.[12]

The effect of geometrical cues on stem cell differentiation have been extensively investigated with different methods (e.g., microcontact printing, lithography, laser machining, etc.) to develop substrates with nanopatterns or micropatterns, such as nanogratings/lanes or microgrooves/lanes.[13,14] Previous reports indicate that cells seeded onto the same square-shaped island with different areas or rectangular-shaped island with different aspect ratios would undergo different lineage commitments.[6,15] It has been suggested that substrate with nanotopography would guide cell differentiation toward neurogenesis.[16,17] For example, poly(dimethylsiloxane) (PDMS) nanogratings could promote stem cell differentiation into neurogenic lineage through the alignment of cytoskeletal actin filament and elongated cell shape.[18,19] The electrospun fibrous scaffold with both random and aligned nanofibers has also been

Received: October 9, 2015
Accepted: December 14, 2015
Published: December 14, 2015

DOI: 10.1021/acsami.5b09588
ACS Appl. Mater. Interfaces 2016, 8, 563−573

Table 1. Compiled List of Gene Targets Probed in This Study

Genebank accession number	gene target	sequence (5′−3′)	amplicon length (bp)
NM 001101	β-actin	CATGTACGTTGCTATCCAGGC CTCCTTAATGTCACGCACGAT	250
NM 002046	GAPDH	CATGAGAAGTATGACAACAGCCT AGTCCTTCCACGATACCAAAGT	113
NM 000364	Cardiac troponin I (cTnI)	TCTCCGAAACAGGATCAACGA GCCCGGTGACTTTAGCCTT	68
NM 002052	GATA-4	CCCAGACGTTCTCAGTCAGTG GCTGTTCCAAGAGTCCTGCT	146
NM 002478	MyoD1	CGGCGGAACTGCTACGAAG GCGACTCAGAAGGCACGTC	172
NM 000257	β-Myosin Heavy Chain (MHC)	CACTGATAACGCTTTTGATGTGC TAGGCAGACTTGTCAGCCTCT	165
NM 006086	Class III β-Tublin	GGCCAAGGGTCACTACACG GCAGTCGCAGTTTTCACACTC	85
X65964	Nestin	CAACAGCGACGGAGGTCTC CCTCTACGCTCTCTTCTTTGAGT	163
NM 002500	NeuroD1	GCCTTGCTATTCTAAGACGCA GTGGGTTGGGATAAGCCCTT	156
NM 002374	Microtubule Associated Protein (MAP2)	CAGGAATTGACTCCCTCTACAGC TCTTCACCAGGCTTACTTTGC	80

shown to enhance nerve regeneration.[20,21] While exploring the micropatterned fibronectin strips in driving stem cell myogenesis,[22−26] we found that micropatterns with 20-μm-wide fibronectin strips caused cytoskeleton rearrangement and cell elongation, which exerted significant impact on directing stem cell fate toward myogenic lineage.[24,27] In particular, we observe that aligned stem cells on this micropatterned platform could predominantly induce myogenesis of MSCs from different sources, as proved by the significant increase of myogenic transcription factors and positive immunofluorescent labeling of the myogenic marker.[26] Therefore, it is critical to investigate the responses of stem cells when they are in spontaneously stimulated with microscopic to submicroscopic geometrical cues.

In this study, we designed and fabricated micropatterned hybrid grafts and investigated its influence on human mesenchymal stem cell (hMSC) differentiation in the absence of biochemical inducers. The fibronectin lanes were micropatterned on solution electrospun fibrous mats with random or aligned fibers. There are several methods to fabricate fibrous mats, including solution electrospinning and melt spinning. Melt spinning avoids toxic solvents present in the spinning process; however, a fiber diameter of 5−25 μm is a more typical range for melt spinning fibrous mats.[28] The angles between the aligned fibers and micropatterns was varied from 0° to 45° to 90°. Here, we demonstrated that both micropatterns on random and aligned electrospun fibrous mats modulated hMSCs toward neural-like cells. We further showed that micropatterns with an angle of 45° could largely promote neurogenesis of hMSCs without addition of biochemical cues, as verified by qRT-PCR and immunostaining. A significantly elevated mRNA levels of neurogenic markers including MAP2, Nestin, NeuroD1, and Class III β-Tubulin were detected. Moreover, neurogenic lineage differentiation of hMSCs was confirmed by immunostaining of MAP2 at the protein level.

EXPERIMENTAL SECTION

Preparation of Solid Film Substrates and Porous Mats. The solid poly(L-lactide-*co*-ε-caprolactone) (PLC) (70:30, Purac Biomaterials, Lincolnshire, IL) films were fabricated by the solvent casting method. PLC granules were dissolved in dichloromethane (Tedia, Fairfield, OH) at a mass-to-volume ratio of 1:5 to achieve an optimal viscosity that is suitable for the solvent casting process. The PLC films were cast using an industrial film applicator (Paul N. Gardner Company, Inc., Sheen automatic film applicator, Pompano Beach, FL, USA). The films were allowed to stand in a vacuum oven at 37 °C for 5 d to completely remove the residual solvent. The thickness of the dry films was measured using a thickness gauge (Elcometer).

The porous mats were fabricated using an electrospinning technique. The PLC polymer solutions were prepared in a solvent mixture of dichloromethane and *N*,*N*-dimethyl formamide in a 4:1 volume ratio. The porous electrospun mats with random fibers were produced by dispensing the polymer solution at a flow rate of 1 mL/h under a voltage of 15 kV using NANON-01A (MECC Co., Ltd., Fukuoka, Japan). The porous electrospun mats with aligned fibers were obtained under the same condition; however, a disk collector was used with a rotation speed of 1500 rpm. The distances between the polymer supply to the collectors are 12 cm in both cases. The morphologies of electrospun mats were examined by scanning electron microscopy (SEM). The cross section of mats were archived through freeze-fracture in liquid nitrogen.[29]

Construction of Micropatterned Substrates. A microcontact printing method was used to transfer ECM protein, fibronectin, onto

DOI: 10.1021/acsami.5b09588
ACS Appl. Mater. Interfaces 2016, 8, 563−573

Scheme 1. Schematic Representation of the Fabrication Procedures for Micropatterning on Fibrous Mats Using Electrospinning and Microcontact Printing Techniques

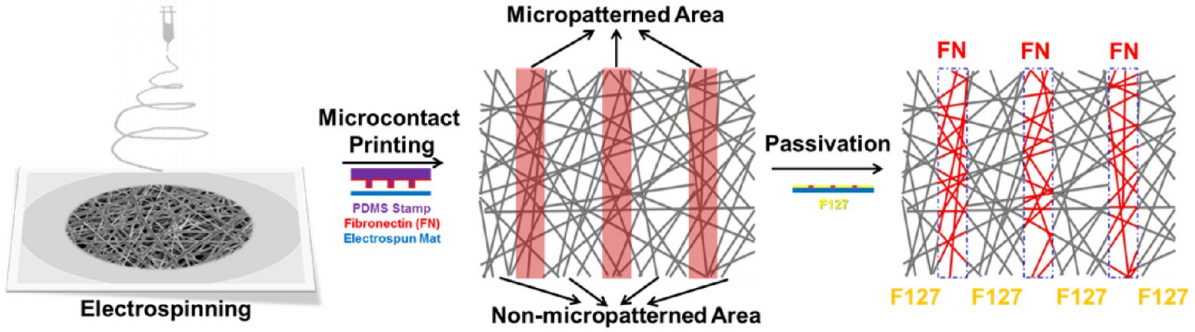

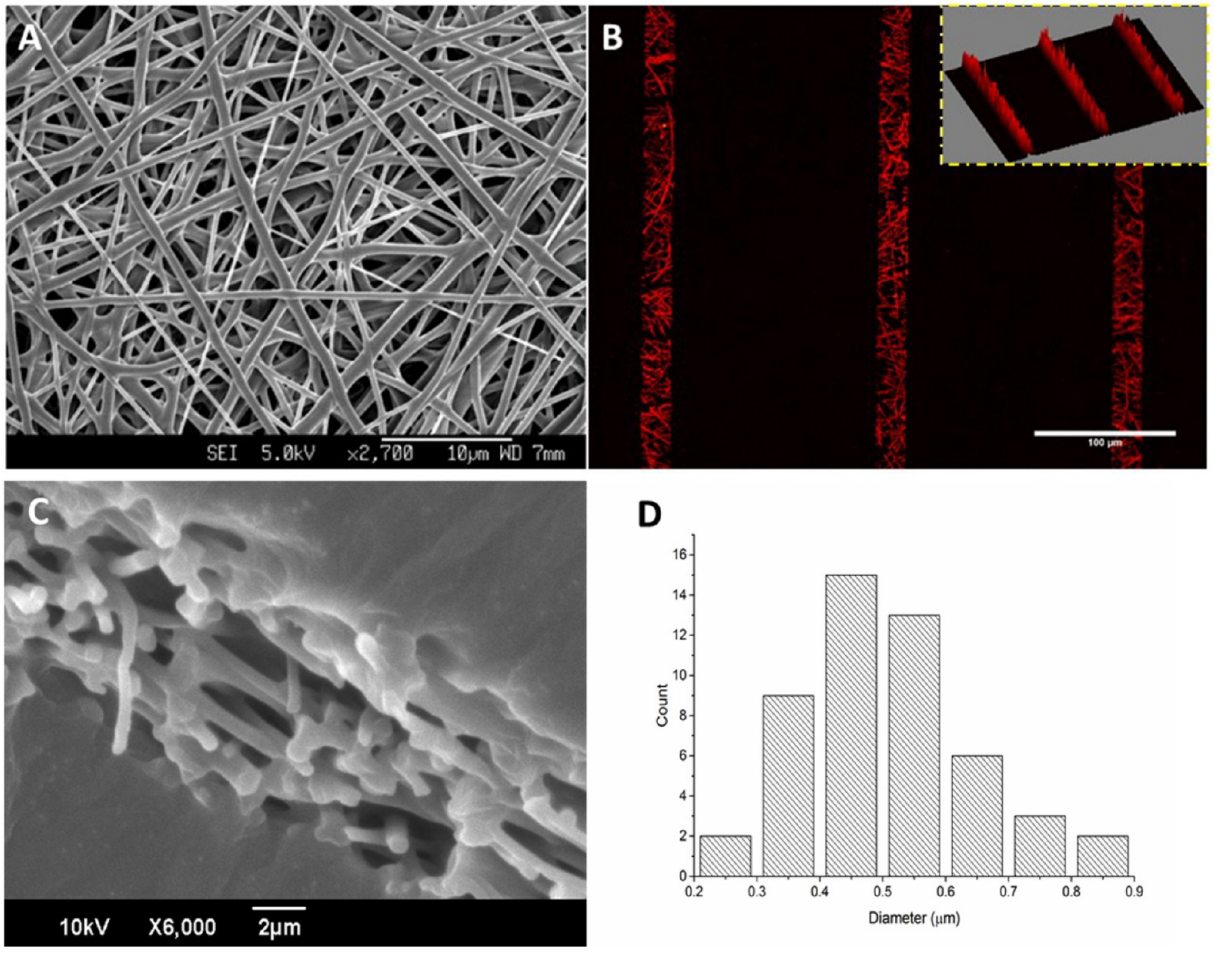

Figure 1. Representative images of electrospun fibrous mat shown by (A) SEM and (B) micropatterned fibrous hybrid graft showed by immunofluorescence labeling of fibronectin lanes. Inset in panel (B) shows a 3D reconstruction of textured protein features on the surface of the hybrid graft using ImageJ software; red peaks represent the density of imprinted ECM protein. (C) SEM micrographs of the freeze-fracture cross section of random electrospun fibrous mat showing the diameter of fibers. (D) Histogram of fiber diameter illustrated the distribution of fiber diameter in fibrous mat.

the substrates, as mentioned previously.[24,27] Briefly, polydimethylsiloxane (PDMS) elastomeric stamps with desired topographic features were first fabricated using a standard photolithography method. After the ECM protein solution was ink-incubated on the PDMS stamps for 1 h at room temperature, PDMS stamps were blown dried using pressurized purified nitrogen gas. Then the conformal contact of PDMS stamps and PCL substrates for 30 min at room temperature will transfer print the fibronectin lane patterns onto the substrates. Pluronic F127 (2.5w/v% in PBS) was used to passivate the nonprinting area for 1 h at 37 °C. Excess F127 was washed away by PBS before cell seeding. Immuno-labeling of fibronectin lanes with rabbit polyclonal antifibronectin (1:400, Sigma−Aldrich) and staining with Cy3 goat antirabbit IgG (1:400, Millipore) were applied to verify the geometry of micropatterned fibronectin lanes. In addition to immunostaining of fibronectin, the fibronectin ink printed mat were examined via Fourier transform infrared (FTIR) spectroscopy. FTIR spectra of PLC mat and fibronectin printed mat were measured on a Perkin−Elmer Spectrum GX FTIR spectrometer (Perkin−Elmer, Inc., Waltham, MA, USA).

DOI: 10.1021/acsami.5b09588
ACS Appl. Mater. Interfaces 2016, 8, 563−573

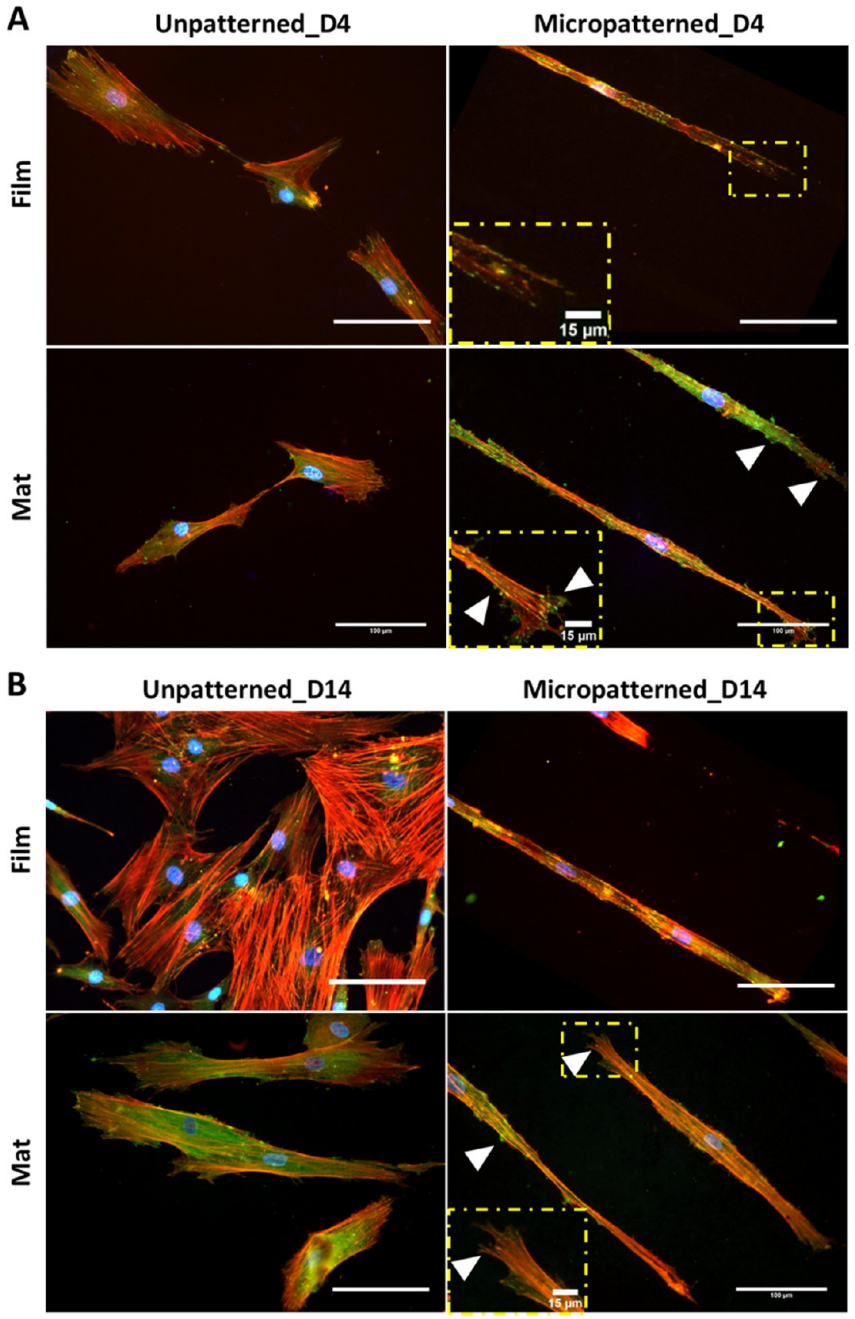

Figure 2. Merged images of immunofluorescence staining of hMSCs with phalloidin for microfilament (F-actin, red), vinculin for focal adhesion complex (green) and DAPI for nucleus (blue), on the respective substrates (film control, mat control, micropatterned film substrates, and micropatterned mat substrates) after culture for (A) 4 days and (B) 14 days. Inset shows the growth of conelike structures that were found on cells cultured on micropatterned mat substrates. Scale bar = 100 μm.

Cell Culture. The hMSCs and cell culture medium were both obtained from Lonza (Cambrex, U.K.). Cells are guaranteed to express CD29, CD44, CD105, and CD166 and to not express CD14, CD34, and CD45. All lots of this product are also guaranteed to express CD90 and CD73 and to not express HLA-DR or CD19. Cells were expanded and cultured in MSC growth medium, according to the vendor's instruction (Lonza, Cambrex, U.K.). Culture medium was changed every 2−3 days. PBS and 0.05% trypsin-EDTA (Invitrogen) were used for washing and cell detachment purposes, respectively. After cells were harvested and seeded onto experimental substrates, cells were cultured with low-glucose Dulbecco's Modified Eagle's Medium (DMEM) containing L-glutamine (Sigma−Aldrich, USA) supplemented with 10% fetal bovine serum (FBS) (PAA, Pasching, Austria), and 1% antibiotic/antimycotic solution (PAA, Pasching, Austria) hMSCs were seeded at a density of 650 cells/cm^2 on the patterned and unpatterned substrates. At the end of 30 min of incubation, unattached cells were washed off by introducing fresh culture medium.

Immunocytochemistry and Microscopy. In brief, cells cultured on the substrates after 4 and 14 days were fixed with 4% paraformaldehyde for 15 min and then permeabilized with 0.1% Triton X-100 for 5 min and followed by blocking with 5% bovine serum albumin (BSA, Sigma−Aldrich) or 5% goat serum (Sigma−Aldrich). The primary antibodies used to target interested proteins were vinculin, microtubule-associated proteins 2 (MAP2), Myosin Heavy Chain (MHC), and fibronectin. Secondary antibodies used were Alexa Fluor 488 goat antimouse, Alexa Fluor 568 goat antichicken, and Cy3 goat antirabbit IgG (1:400, Millipore). C2C12

DOI: 10.1021/acsami.5b09588
ACS Appl. Mater. Interfaces 2016, 8, 563−573

myoblast and neural stem cell were used as positive controls for MHC and MAP2 staining, respectively. Filamentous actin (F-actin) and nucleus were stained with tetramethylrhodamine isothiocyanate (TRITC)-conjugated phalloidin (1:800, Chemicon) and 4′,6-diamidino-2-phenylindole (DAPI) (Invitrogen, 1:1000), respectively. Negative controls in the absence of primary antibodies were also performed. Fluorescence images were visualized with a Nikon 80i eclipse (Nikon, Japan) upright microscope and captured with the Nikon DS-Fi1 camera (Nikon, Japan), using two 20× and 40× objective lenses.

Quantitative Real-Time Polymerase Chain Reaction (qRT-PCR). Total RNA was isolated using RNeasy Mini Kit (Qiagen, USA) according to the vendor's instructions. An amount of 0.1−0.5 μg of total RNA was used to synthesize complementary DNA (cDNA) with a reverse transcription kit (Bio-Rad). The real-time reaction was performed on a CFX96 RT-PCR detection system (Bio-Rad Lab, Inc.) with KAPA SYBR Green Fast Master mix. Primer sequences of housekeeping and specific genes were selected from Primer Bank (http://pga.mgh.harvard.edu/primerbank/), as listed in Table 1.[30] The expression of target genes was normalized to GAPDH and β-actin, using Relative Expression Software Tool (REST) software.[31] The results presented here in the form of a two-dimensional (2D) heat map, where the scale of the heat map—green to red—indicates lowest to highest fold changes.

Statistical Analysis. All experiments were repeated thrice with at least triplicate samples in each run. All data are presented as mean ± standard deviation (SD). Statistical analysis was carried out using one-way analysis of variance (ANOVA), and the values are considered significantly different when $p < 0.05$.

RESULTS AND DISCUSSION

Fabrication of Micropatterned Hybrid Grafts. A microcontact printing method has been used to pattern many different types of materials, including self-assembled monolayers, proteins, and DNA,[32,33] which is widely used in understanding how cells respond to the patterned substrates.[34−36] Our previous work have shown that micropatterned bioresorbable PLGA film substrate could reorganize cells to mimic the *in vivo* cell orientation of myocardium, which provides a possible platform for myocardial tissue engineering.[24,27] Here, fibronectin lanes were microimprinted onto an electrospun fibrous substrate and the response of cells to both micro and submicro geometric cues were investigated. The schematic representation of the fabrication procedures for micropatterning were illustrated in Scheme 1. First, a polymeric fibrous PLC mat was fabricated by electrospinning a polymeric solution onto a collection target. Electrospinning generated PLC substrates consists of nonwoven fibrous mats, with an average fiber diameter of 530 ± 60 nm (see Figures 1A, 1C, and 1D, as well as Figures 4A, 4E, and 4F). Second, fibronectin lanes were ink-printed onto the electrospun fibrous mats by microcontact printing. which was revealed by FTIR spectra (see Figure S1 in the Supporting Information). The intense band at 1746 cm^{-1} corresponding to the carbonyl stretch C═O of the carboxyl functional group of PLC in the two spectra. However, one distinct bands was observed at 3419 cm^{-1} in inked PLC mat spectrum. The broad band at 3419 cm^{-1} corresponds to N−H stretch of primary and secondary amines in fibronectin.[37] The FTIR spectrum suggested that the fibronectin were successfully inked onto the surface of PLC mat. The uniformly distributed fluorescence intensity of printed fibronectin lanes as revealed by immunostaining across the porous mats surface testified the quality of the transferred specific ECM protein (Figure 1B). Finally, the passivation of nonmicropatterned area using Pluronic F127 was done for site-selective cell growth. The inclusion of nonfouling agents to block the nonspecific protein adsorption would result in the precise spatial control of cell adhesion, migration, and maintenance of cell morphology within the micropatterns.

Cellular Morphology Analysis and Differentiation Study of hMSCs Cultured on Micropatterned Hybrid Grafts with Randomly Distributed Fibers. In order to examine the cell morphology, microfilament rearrangement, and focal adhesion development caused by micropatterns, immunofluorescence staining of hMSCs with phalloidin for microfilament (F-actin, red), vinculin for focal adhesion complex (green) and DAPI for nucleus (blue), on the respective substrates (film control, mat control, micropatterned film substrates, and micropatterned mat substrates) after culture for 4 and 14 days are illustrated in Figure 2. Two fibrous mat substrates were made of randomly oriented fibers. Generally, the cells cultured on unpatterned substrates were well spread out with distinct bundles of well-defined F-actin or stress fibers. Focal adhesions were localized at the cell periphery, or at the end of microfilament or ventral to the cell nucleus. When compared with the control samples, cells on micropatterns seemed to result in less-defined vinculin. Cells cultured on both micropatterned film and fibrous mat substrates showed increased cellular alignment along the direction of fibronectin lanes. The highly organized stress fiber bundles were stretched along the long axis of cells. Interestingly, a higher occurrence of the protrusive subcellular features, such as filopodia, was found on cells cultured on a micropatterned fibrous mat substrate, compared to micropatterned film. This type of feature is similar to the specialized growth cone structure, which is usually located at the very tip of the highly motile neural cellular structures (i.e., growing axons and dendrites).[38] Filopodia is a characteristic for cells exhibiting exploratory behavior, especially for neuronal cells and typically appeared as the fine extension of the growth cone. While cells on the micropatterned film substrate were characterized to show the presence of cell membrane at the edges in general, an extensive formation of filopodia was revealed for the cells cultured on the micropatterned fibrous mat substrate. Filopodia is one of the cell's main sensory tools and especially has been demonstrated to probe nanotopography, such as nanopits and carbon nanotubes.[25,39] One of the key functions of filopodia is to promote cell motility through sensing surrounding microenvironment using filopodia contained receptors. The cytoskeletal actin bundles drive the formation of filopodia. Once it encounters a favorable guidance cue, the stabilization of filopodia happened and cells start to recruit microtubules and accumulate actins.[40] After cells locate a suitable feature using their filopodia, lamelliopodium are formed. As shown in the images (Figure 2, white arrow), comparatively more filopodia formation was caused by electrospun fiber guidance on cell cultured on micropatterned fibrous mat substrate at day 4, not only at both ends of cells, but also along both edges of micropatterns. Less filopodia formation was found for the cells cultured on micropatterned fibrous mat substrate after 14 days. The presence of growth conelike structure is one remarkable morphology of neurite. As mentioned beforehand, microscale and nanoscale geometric cues may affect stem cell differentiation toward different lineages when cells experience obvious, macroscopic alteration in cell shape.[11,41−44] The stretched and elongated cell shape seems to be conducive for both neurogenic and myogenic gene expressions. Thus, it is important to further correlate morphological changes to the changes in cell lineage commitment.

DOI: 10.1021/acsami.5b09588
ACS Appl. Mater. Interfaces 2016, 8, 563−573

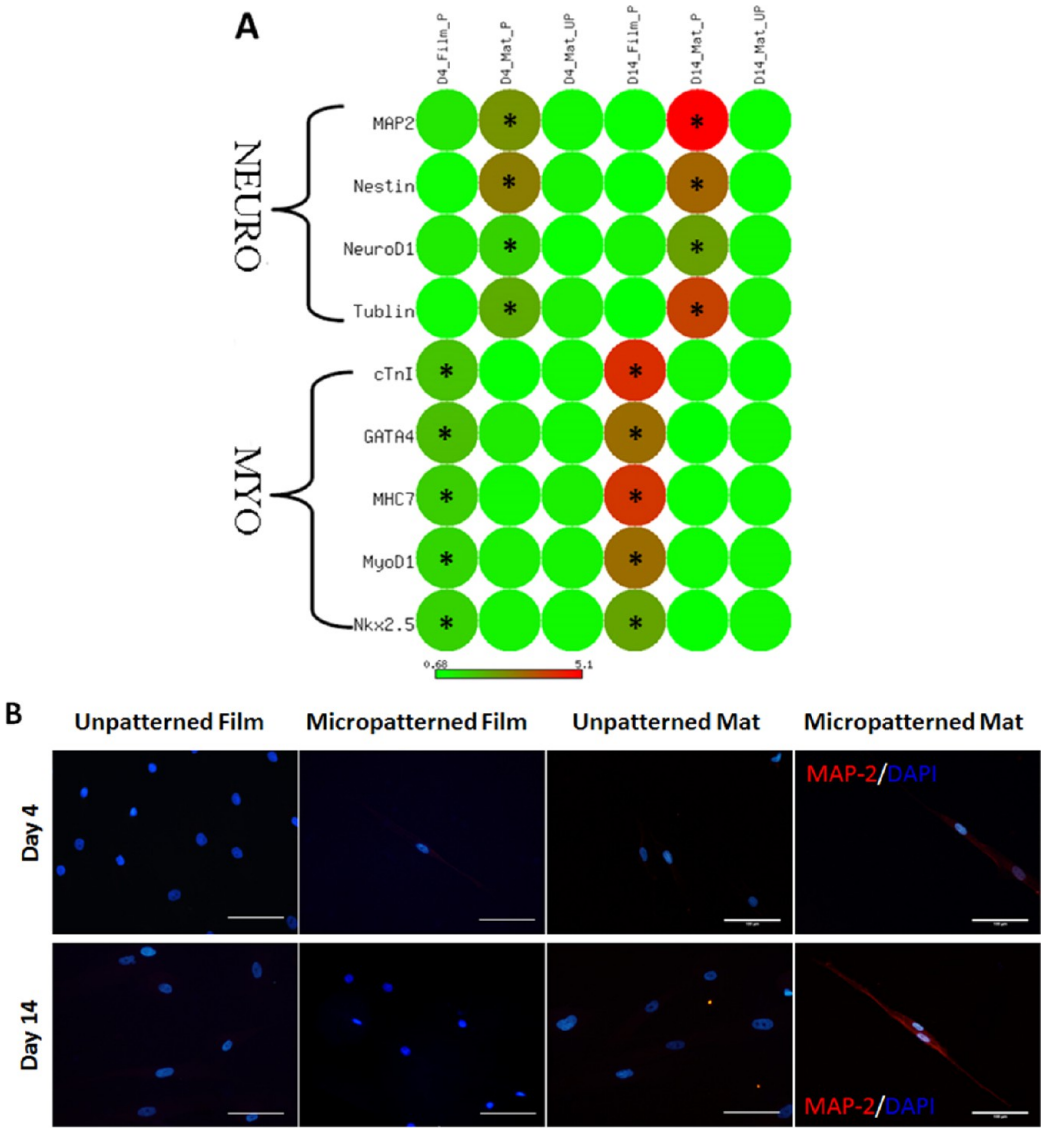

Figure 3. Micropatterned hybrid graft-induced cytoskeleton rearrangement lead to the activation of selective neurogenic specific markers: (A) qPCR results of the relative mRNA transcripts expression levels of the patterned cells normalized to the control group of unpatterned substrates after 4 and 14 days is illustrated in the form of heat map (asterisk (*) denotes $p < 0.05$; the quantitative data of qPCR are shown in Table S1 in the Supporting Information); (B) significant neurogenic marker MAP2 (red) was immunodetected in the micropatterned mats group after 14 days but not for the micropatterned film group and unpatterned control cells. Scale bar = 100 μm.

We have previously shown that micropatterned fibronectin lanes on film substrate could lead to the expression of myogenic genes and up-regulation of myocardiac-specific protein (Myosin Heavy Chain, MHC) via the cellular elongation caused by micropatterns.[24,27] Meanwhile, negligible neurogenic gene expressions were observed, although expression at protein level was not detected. Similarly, real-time quantitative PCR experiments were designed to evaluate the gene expression profiles of myogenic and neurogenic differentiation of hMSCs cultured on micropatterned fibrous mat substrates at two different time points (i.e., day 4 and day 14). Relative gene expression level is reflected in the heat map generated by Matrix2png, with red representing high values of expression and green representing low values of expression.[45] As shown in Figure 3A, while micropatterned film substrate promoted upregulation of myogenic markers in hMSCs after day 4 of subculture, cell neurogenesis was more favorable for those seeded on micropatterned fibrous mat substrates. Significant upregulation of myogenic markers of cTnI, GATA4, MHC7, MyoD1, and Nkx2.5 with 4.3-, 3.3-, 4.1-, 3.2-, and 2.3-fold higher, respectively, were found for cells cultured on micropatterned film substrate at day 14 (relative to the control group of unpatterned film), which showed similar trend on cell myogenesis as reported previously.[27] In contrast, in the cells seeded onto the micropatterned fibrous mat substrate, the mRNA expression levels of early neural markers (Nestin, NeuroD1) and mature neural markers (MAP2, Tubulin) were increased significantly after 14 days of cell culture, when compared to the unpatterned surface. Nestin is reported to be a transient neurogenic marker in multipotential neural stem cells preparing for neural development in early stage[46,47] and the first NeuroD family (D1−D3) to be expressed in neural development is NeuroD1.[48] Both early neuronal differentiation markers were significantly upregulated (Nestin, ∼2.99-fold at day 4 and ∼3.37-fold at day 14; NeuroD1, ∼1.60-fold at day 5 and ∼2.41-fold at day 14) in hMSCs cultured on the

DOI: 10.1021/acsami.5b09588
ACS Appl. Mater. Interfaces 2016, 8, 563−573

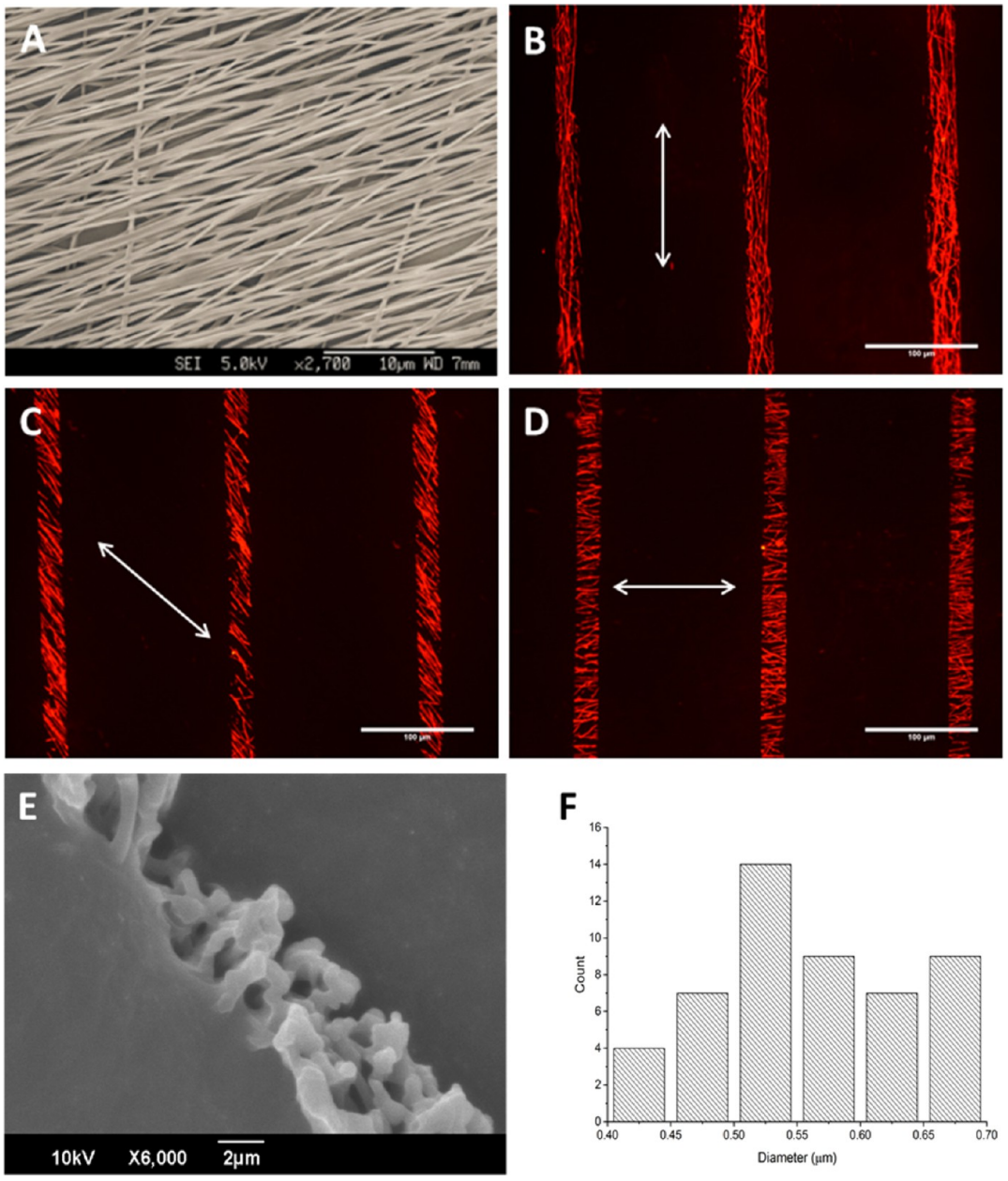

Figure 4. (A) Representative images of electrospun fibrous mat with aligned fibers showed by SEM. Also provided are images of the micropatterned fibrous hybrid graft shown by immunofluorescence labeling of fibronectin lanes (red) with an angle between micropattern and aligned fibers of (B) 0°, (C) 45°, and (D) 90° (scale bar = 100 μm). (E) SEM micrographs of the freeze-fracture cross section of aligned electrospun fibrous mat, showing the diameter of fibers. (F) Histogram of fiber diameter illustrating the distribution of fiber diameter in the fibrous mat.

micropatterned fibrous mat substrate compared to the hMSCs cultured on the mat control substrate. For both mature neuronal markers, MAP2 and Tubulin,[49,50] also presented a high upregulation in gene expression level on both time points consistently. Remarkably, greater expression levels of these genes were found at day 14, as compared to day 4 (day 4, MAP2, 2.62-fold; Tubulin, ∼2.20-fold; day 14, MAP2, ∼5.06-fold, Tubulin ∼3.92-fold). These results clearly indicated that neurogenesis-related genes could be modulated by regulating the cell morphology on the micropatterned fibrous mat substrate. To further analyze hMSCs differentiation, cells were immunostained for MAP2. Only the hMSCs on the micropatterned fibrous mat substrate were stained positive for MAP2, in comparison to the cells on both control substrates and micropatterned film substrates (Figure 3B). Furthermore, no MHC expression was detected for cells on micropatterned fibrous mat substrates, whereas significant MHC staining was observed on cells cultured on micropatterned film substrates (see Figure S1). These results suggested that micropattern lanes on electrospun fibrous mat substrates can promote hMSCs differentiation toward neuronal lineage in exogenous soluble-factor-free conditions through the modulation of micropattern-driven cellular elongation and fiber-engendered filopodia development.

Effect of Angle between Micropatterning and Fiber Orientation on hMSC Behavior. Although randomly distributed fibers on the micropatterned fibrous mat substrate stimulate hMSCs neurogenic differentiation through the inspired protrusion of filopodia, it is unclear whether the orientation of electrospun fibers could further influence cell

DOI: 10.1021/acsami.5b09588
ACS Appl. Mater. Interfaces 2016, 8, 563−573

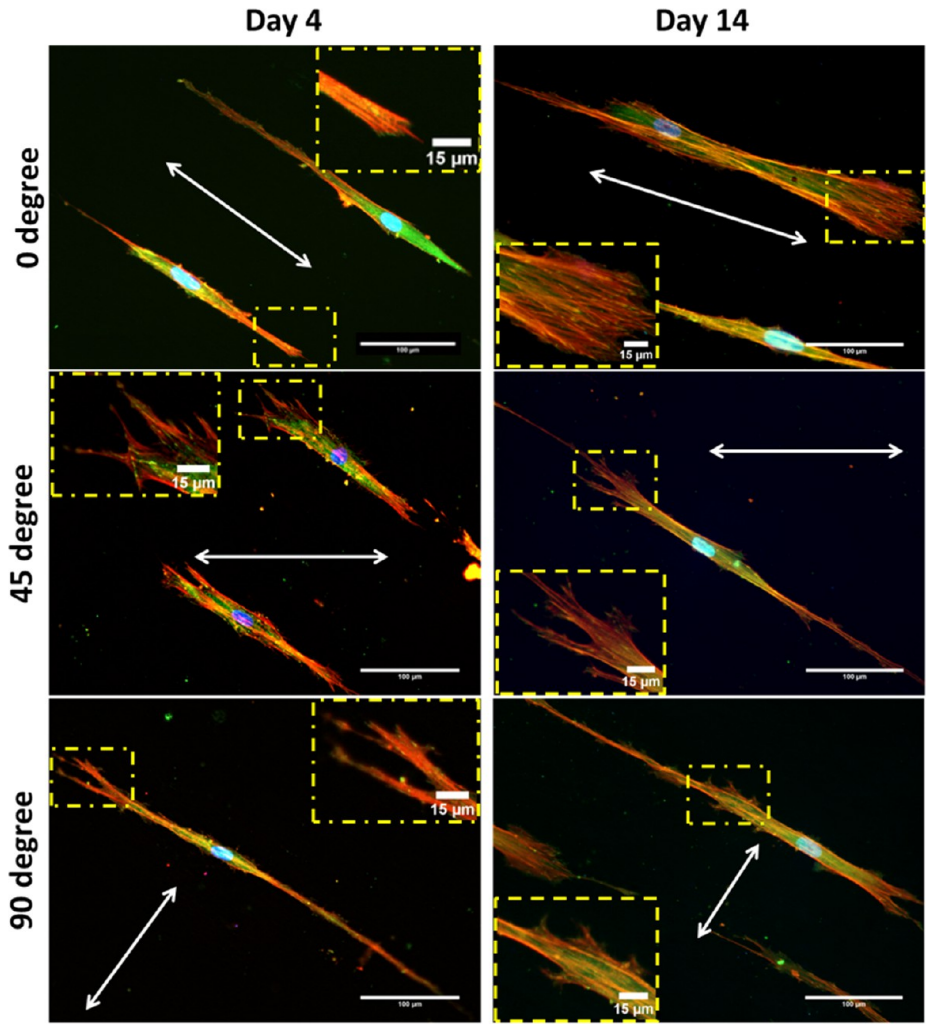

Figure 5. Merged images of immunofluorescence staining of hMSCs with phalloidin for microfilament (F-actin, red), vinculin for focal adhesion complex (green), and DAPI for nucleus (blue), on the micropatterned fibronectin lanes on aligned electrospun fiber mats with the angle between micropattern and aligned fibers of 0°, 45°, and 90° after culture for 4 and 14 days. Scale bar = 100 μm.

differentiation. We deployed the same protocol mentioned above, but made use of aligned electrospun fibrous mats. The micropatterned fibrous hybrid grafts were constructed with different angles between aligned fibers and micropatterns varying at 0°, 45°, and 90° (see Figure 4). Immunostaining of cytoskeletal elements of the micropatterned hMSCs on hybrid grafts (Figure 5) indicated that, for an angle of 0° (fibers aligned with the micropattern), the microfilaments were parallel to the fiber orientation. For an angle of 45°, while the majority of filopodia outgrowth was located at both ends of cells, branches were seen along both edges of each micropattern for cells cultured at an angle of 90°.

As demonstrated previously, micropatterned fibrous mat could cause the formation of growth conelike structure, which gave rise to the upregulation of neurogenic transcript level. Herein, to investigate the influence of varying angle between micropatterning and aligned fibers on hMSCs toward neurogenic differentiation, qPCR was performed to analyze the expression of selective neurogenesis transcript markers. Neurogenic markers expression of hMSCs on micropatterned groups was upregulated significantly after 14 days of culture, compared to its unpatterned controls (Figure 6A). Micropatterned fibrous hybrid graft with an angle of 45° displayed the highest upregulation among the three groups. . The presence of MAP2 could be demonstrated in differentiated hMSCs on all, through micropatterned aligned fibrous mats (Figure 6B). The strongest signal was detected in cells cultured on micropatterned fibrous hybrid graft with an angle of 45°, which implied that neurogenesis of hMSCs favored this type of hybrid graft the most. Since all micropatterned substrates have similar fibrous topography and protein-coated chemistry, it is believed that the angle between the direction of micropatterning and orientation of aligned fibers could be the dominant factor here in affecting the neurogenic upregulation. One possible mechanism for this interesting phenomenon may be extrapolated by the differential location and development of filopodial extensions, as exhibited earlier in this study.

It is established that filopodia, which are formed of tightly bundled actin filaments, plays an important role in many cellular process, such as cell migration, cell adhesion, wound healing, and neurite outgrowth, and serve as precursors for dendritic spines in neurons.[51] Cell adhesion molecules, known as integrins, are normally express in the tips of filopodia.[52,53] It is well-known that cell migration, proliferation, differentiation, and survival are regulated by integrin signaling pathways.[54,55] For example, integrin β1 involved an important signaling mechanism that contributed to maintain neural stem cell behavior.[56] Our previous report also demonstrated that single-

DOI: 10.1021/acsami.5b09588
ACS Appl. Mater. Interfaces 2016, 8, 563−573

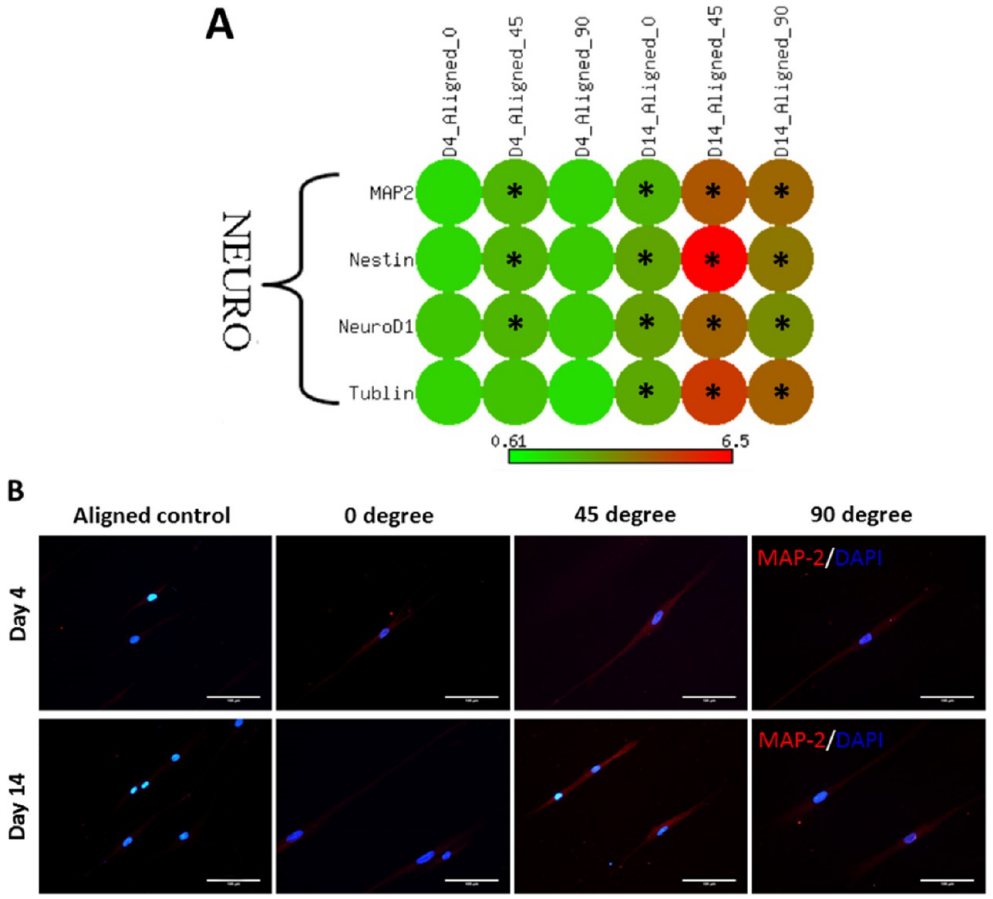

Figure 6. Activation of neurogenic specific markers, as a result of enforced cytoskeleton rearrangement: (A) qPCR results of relative mRNA transcript expression levels of micropatterned cells are presented in the form of heat map (an unpatterned electrospun fibrous mat with aligned fibers was used as a control; $*p < 0.05$). The quantitative data of qPCR are shown in Table S2 in the Supporting Information. (B) Significant neurogenic marker MAP2 (red) was immunodetected in the micropatterned mats group after 14 days but not for the micropatterned film group and unpatterned control cells. Scale bar = 100 μm.

walled carbon nanotubes could commit hMSCs differentiation into neuronal lineage through the modulation of focal adhesions, which are usually integrin-containing multiprotein structures.[25] Modulation of focal adhesion, together with significantly recruited β3 integrin cluster, initiated MLCK and FAK pathways to further promote actin polymerization and create contraction along the actin, and then influence cell behavior, such cell adhesion, spreading, and differentiation.[53,57,58] Another study has demonstrated that, by inhibition of the Arp2/3 complex (a necessary component for filopodia formation), neuritogenesis was affected during neuronal differentiation through Rho GTPases.[59] Altogether, it is conceivable that focal adhesion formation associated with filopodia development, plays an essential role in directing stem cell neurogenesis.

CONCLUSIONS

Investigation of cell fate modulated using physical microenvironmental cues is on the rise, because of the possible side effects caused by biochemical factors, as well as increasing demand on active and smart scaffold for therapeutic treatment. Our study developed a novel approach on the combination of microcontact printing and electrospinning to create a micropatterned hybrid graft for assessing the potential ability of hMSCs differentiation to neuronal commitment without any biochemical inducers. The distinctive morphological change, as well as enhanced filopodia development of the cultured human mesenchymal stem cells (hMSCs), is significantly influenced by a combination of micropattern and fibrous topography, that subsequently triggered the expression of early neural phenotypic markers, nestin, and Class III β-tubulin, thereby transforming hMSCs to neural-like cells on hybrid constructs. Of particular interest is the angle between the micropatterning and fiber orientation that affected cell behavior in a totally unexpected way. An angle of 45° could largely stimulate filopodia (growth of a conelike structure) branching outgrowth, and neurogenesis of hMSCs. Overall, this work demonstrates the potential of micropatterned hybrid scaffold as an effective physical cue to promote early neural-like differentiation of stem cells *in vitro*, thus providing an insight into future development of engineered functionalized porous micropatterned medical device design and its application in neural tissue engineering.

ASSOCIATED CONTENT

Supporting Information

The Supporting Information is available free of charge on the ACS Publications website at DOI: 10.1021/acsami.5b09588.

FTIR spectra for PLC fibrous mat and fibronectin ink printed fibrous mat (Figure S1). Immunostaining of MHC expression was assessed for cells on control groups, micropatterned fibrous mat substrates and micropatterned film substrates (Figure S2). The relative

DOI: 10.1021/acsami.5b09588
ACS Appl. Mater. Interfaces 2016, 8, 563−573

quantification of gene expression (Tables S1 and S2) (PDF)

AUTHOR INFORMATION

Corresponding Authors

*Tel.: +86 577 88017557. Fax: +86 577 88017508. E-mail: lihq@wibe.ac.cn.

*Tel.: +65 67906186. Fax: +65 67909081. E-mail: lptan@ntu.edu.sg.

Notes

The authors declare no competing financial interest.

ACKNOWLEDGMENTS

The authors gratefully acknowledge financial support from Nanyang Technological University Tier 1 (Grant No. RGT24/13) and Wenzhou government's start-up fund (Grant No. WIBEZD2014005-01 & Grant No. WIBEZD2014005-04) for Wenzhou Institute of Biomaterials and Engineering.

REFERENCES

(1) Derby, B. Printing and Prototyping of Tissues and Scaffolds. *Science* **2012**, *338*, 921−926.

(2) Lamoureux, P.; Ruthel, G.; Buxbaum, R. E.; Heidemann, S. R. Mechanical Tension Can Specify Axonal Fate in Hippocampal Neurons. *J. Cell Biol.* **2002**, *159*, 499−508.

(3) Mooney, E.; Mackle, J. N.; Blond, D. J. P.; O'Cearbhaill, E.; Shaw, G.; Blau, W. J.; Barry, F. P.; Barron, V.; Murphy, J. M. The Electrical Stimulation of Carbon Nanotubes to Provide a Cardiomimetic Cue to MSCs. *Biomaterials* **2012**, *33*, 6132−6139.

(4) Ventura, C.; Maioli, M.; Asara, Y.; Santoni, D.; Mesirca, P.; Remondini, D.; Bersani, F. Turning on Stem Cell Cardiogenesis with Extremely Low Frequency Magnetic Fields. *FASEB J.* **2005**, *19*, 155−157.

(5) Dalby, M. J.; Gadegaard, N.; Oreffo, R. O. C. Harnessing Nanotopography and Integrin-Matrix Interactions to Influence Stem Cell Fate. *Nat. Mater.* **2014**, *13*, 558−569.

(6) McBeath, R.; Pirone, D. M.; Nelson, C. M.; Bhadriraju, K.; Chen, C. S. Cell Shape, Cytoskeletal Tension, and RhoA Regulate Stem Cell Lineage Commitment. *Dev. Cell* **2004**, *6*, 483−495.

(7) Sanchez-Ramos, J.; Song, S.; Cardozo-Pelaez, F.; Hazzi, C.; Stedeford, T.; Willing, A.; Freeman, T. B.; Saporta, S.; Janssen, W.; Patel, N.; Cooper, D. R.; Sanberg, P. R. Adult Bone Marrow Stromal Cells Differentiate into Neural Cells in Vitro. *Exp. Neurol.* **2000**, *164*, 247−256.

(8) Li, H.; Lai, Y.; Huang, J.; Tang, Y.; Yang, L.; Chen, Z.; Zhang, K.; Wang, X.; Tan, L. P. Multifunctional Wettability Patterns Prepared by Laser Processing on Superhydrophobic TiO_2 Nanostructured Surfaces. *J. Mater. Chem. B* **2015**, *3*, 342−347.

(9) Biggs, M. J. P.; Richards, R. G.; Dalby, M. J. Nanotopographical Modification: A Regulator of Cellular Function through Focal Adhesions. *Nanomedicine (NY, NY, U. S.)* **2010**, *6*, 619−633.

(10) Dalby, M. J.; Gadegaard, N.; Herzyk, P.; Sutherland, D.; Agheli, H.; Wilkinson, C. D. W.; Curtis, A. S. G. Nanomechanotransduction and Interphase Nuclear Organization Influence on Genomic Control. *J. Cell. Biochem.* **2007**, *102*, 1234−1244.

(11) Guilak, F.; Cohen, D. M.; Estes, B. T.; Gimble, J. M.; Liedtke, W.; Chen, C. S. Control of Stem Cell Fate by Physical Interactions with the Extracellular Matrix. *Cell Stem Cell* **2009**, *5*, 17−26.

(12) Biggs, M. J. P.; Richards, R. G.; Gadegaard, N.; Wilkinson, C. D. W.; Oreffo, R. O. C.; Dalby, M. J. The Use of Nanoscale Topography to Modulate the Dynamics of Adhesion Formation in Primary Osteoblasts and ERK/MAPK Signalling in STRO-1+ Enriched Skeletal Stem Cells. *Biomaterials* **2009**, *30*, 5094−5103.

(13) An, J.; Chua, C. K.; Yu, T.; Li, H.; Tan, L. P. Advanced Nanobiomaterial Strategies for the Development of Organized Tissue Engineering Constructs. *Nanomedicine* **2013**, *8*, 591−602.

(14) Wong, Y. S.; Tay, C. Y.; Wen, F.; Venkatraman, S. S.; Tan, L. P. Engineered Polymeric Biomaterials for Tissue Engineering. *Curr. Tissue Eng.* **2012**, *1*, 41−53.

(15) Kilian, K. A.; Bugarija, B.; Lahn, B. T.; Mrksich, M. Geometric Cues for Directing the Differentiation of Mesenchymal Stem Cells. *Proc. Natl. Acad. Sci. U. S. A.* **2010**, *107*, 4872−4877.

(16) Chua, J. S.; Chng, C.-P.; Moe, A. A. K.; Tann, J. Y.; Goh, E. L. K.; Chiam, K.-H.; Yim, E. K. F. Extending Neurites Sense the Depth of the Underlying Topography during Neuronal Differentiation and Contact Guidance. *Biomaterials* **2014**, *35*, 7750−7761.

(17) Ankam, S.; Suryana, M.; Chan, L. Y.; Moe, A. A. K.; Teo, B. K. K.; Law, J. B. K.; Sheetz, M. P.; Low, H. Y.; Yim, E. K. F. Substrate Topography and Size Determine the Fate of Human Embryonic Stem Cells to Neuronal or Glial Lineage. *Acta Biomater.* **2013**, *9*, 4535−4545.

(18) Yim, E. K. F.; Pang, S. W.; Leong, K. W. Synthetic Nanostructures Inducing Differentiation of Human Mesenchymal Stem Cells into Neuronal Lineage. *Exp. Cell Res.* **2007**, *313*, 1820−1829.

(19) Teo, B. K. K.; Wong, S. T.; Lim, C. K.; Kung, T. Y. S.; Yap, C. H.; Ramagopal, Y.; Romer, L. H.; Yim, E. K. F. Nanotopography Modulates Mechanotransduction of Stem Cells and Induces Differentiation through Focal Adhesion Kinase. *ACS Nano* **2013**, *7*, 4785−4798.

(20) Xie, J.; MacEwan, M. R.; Li, X.; Sakiyama-Elbert, S. E.; Xia, Y. Neurite Outgrowth on Nanofiber Scaffolds with Different Orders, Structures, and Surface Properties. *ACS Nano* **2009**, *3*, 1151−1159.

(21) Smith Callahan, L. A.; Xie, S.; Barker, I. A.; Zheng, J.; Reneker, D. H.; Dove, A. P.; Becker, M. L. Directed Differentiation and Neurite Extension of Mouse Embryonic Stem Cell on Aligned Poly(lactide) Nanofibers Functionalized with YIGSR Peptide. *Biomaterials* **2013**, *34*, 9089−9095.

(22) Li, H.; Wen, F.; Wong, Y. S.; Boey, F. Y. C.; Subbu, V. S.; Leong, D. T.; Ng, K. W.; Ng, G. K. L.; Tan, L. P. Direct Laser Machining-induced Topographic Pattern Promotes Up-regulation of Myogenic Markers in Human Mesenchymal Stem Cells. *Acta Biomater.* **2012**, *8*, 531−539.

(23) Li, H.; Wong, Y. S.; Wen, F.; Ng, K. W.; Ng, G. K. L.; Venkatraman, S. S.; Boey, F. Y. C.; Tan, L. P. Human Mesenchymal Stem-Cell Behaviour On Direct Laser Micropatterned Electrospun Scaffolds with Hierarchical Structures. *Macromol. Biosci.* **2013**, *13*, 299−310.

(24) Tay, C. Y.; Pal, M.; Yu, H.; Leong, W. S.; Tan, N. S.; Ng, K. W.; Venkatraman, S.; Boey, F.; Leong, D. T.; Tan, L. P. Bio-inspired Micropatterned Platform to Steer Stem Cell Differentiation. *Small* **2011**, *7*, 1416−1421.

(25) Tay, C. Y.; Gu, H.; Leong, W. S.; Yu, H.; Li, H. Q.; Heng, B. C.; Tantang, H.; Loo, S. C. J.; Li, L. J.; Tan, L. P. Cellular Behavior of Human Mesenchymal Stem Cells Cultured on Single-walled Carbon Nanotube Film. *Carbon* **2010**, *48*, 1095−1104.

(26) Yu, T.; Chua, C. K.; Tay, C. Y.; Wen, F.; Yu, H.; Chan, J. K. Y.; Chong, M. S. K.; Leong, D. T.; Tan, L. P. A Generic Micropatterning Platform to Direct Human Mesenchymal Stem Cells from Different Origins Towards Myogenic Differentiation. *Macromol. Biosci.* **2013**, *13*, 799−807.

(27) Tay, C. Y.; Yu, H.; Pal, M.; Leong, W. S.; Tan, N. S.; Ng, K. W.; Leong, D. T.; Tan, L. P. Micropatterned Matrix Directs Differentiation of Human Mesenchymal Stem Cells towards Myocardial Lineage. *Exp. Cell Res.* **2010**, *316*, 1159−1168.

(28) Brown, T. D.; Edin, F.; Detta, N.; Skelton, A. D.; Hutmacher, D. W.; Dalton, P. D. Melt Electrospinning of Poly(ε-caprolactone) Scaffolds: Phenomenological Observations Associated with Collection and direct Writing. *Mater. Sci. Eng., C* **2014**, *45*, 698−708.

(29) Cipitria, A.; Skelton, A.; Dargaville, T. R.; Dalton, P. D.; Hutmacher, D. W. Design, Fabrication and Characterization of PCL Electrospun Scaffolds—A Review. *J. Mater. Chem.* **2011**, *21*, 9419−9453.

(30) Spandidos, A.; Wang, X.; Wang, H.; Seed, B. PrimerBank: A Resource of Human and Mouse PCR Primer Pairs for Gene

DOI: 10.1021/acsami.5b09588
ACS Appl. Mater. Interfaces 2016, 8, 563−573

Expression Detection and Quantification. *Nucleic Acids Res.* **2010**, *38*, D792−799.
(31) Pfaffl, M. W.; Horgan, G. W.; Dempfle, L. Relative Expression Software Tool (REST) for Group-wise Comparison and Statistical Analysis of Relative Expression Results in Real-time PCR. *Nucleic Acids Res.* **2002**, *30*, E36.
(32) Yu, H.; Xiong, S.; Tay, C. Y.; Leong, W. S.; Tan, L. P. A Novel and Simple Microcontact Printing Technique for Tacky, Soft Substrates and/or Complex Surfaces in Soft Tissue Engineering. *Acta Biomater.* **2012**, *8*, 1267.
(33) Alom Ruiz, S.; Chen, C. S. Microcontact Printing: A Tool to Pattern. *Soft Matter* **2007**, *3*, 168−177.
(34) Singhvi, R.; Kumar, A.; Lopez, G.; Stephanopoulos, G.; Wang, D.; Whitesides, G.; Ingber, D. Engineering Cell Dhape and Function. *Science* **1994**, *264*, 696−698.
(35) Thery, M.; Racine, V.; Pepin, A.; Piel, M.; Chen, Y.; Sibarita, J.-B.; Bornens, M. The Extracellular Matrix Guides the Orientation of the Cell Division Axis. *Nat. Cell Biol.* **2005**, *7*, 947−953.
(36) Nelson, C. M.; Jean, R. P.; Tan, J. L.; Liu, W. F.; Sniadecki, N. J.; Spector, A. A.; Chen, C. S. Emergent Patterns of Growth Controlled by Multicellular Form and Mechanics. *Proc. Natl. Acad. Sci. U. S. A.* **2005**, *102*, 11594−11599.
(37) Wen, F.; Wong, H. K.; Tay, C. Y.; Yu, H.; Li, H.; Yu, T.; Tijore, A.; Boey, F. Y.; Venkatraman, S. S.; Tan, L.P. Induction of Myogenic Differentiation of Human Mesenchymal Stem Cells Cultured on Notch Agonist (Jagged-1) Modified Biodegradable Scaffold Surface. *ACS Appl. Mater. Interfaces* **2014**, *6*, 1652−1661.
(38) Bray, D.; Bunge, M. B. The Growth Cone in Neurite Extension. In *Locomotion of Tissue Cells*; Ciba Foundation Symposium, No. *14*; Associated Scientific Publishers: New York, 1973; pp 195−209.
(39) Dalby, M. J.; Gadegaard, N.; Riehle, M. O.; Wilkinson, C. D. W.; Curtis, A. S. G. Investigating Filopodia Sensing using Arrays of Defined Nano-pits Down to 35 nm Diameter in Size. *Int. J. Biochem. Cell Biol.* **2004**, *36*, 2005−2015.
(40) Lin, C. H.; Forscher, P. Cytoskeletal Remodeling during Growth Cone−Target Interactions. *J. Cell Biol.* **1993**, *121*, 1369−1383.
(41) Kulangara, K.; Leong, K. W. Substrate Topography Shapes Cell Function. *Soft Matter* **2009**, *5*, 4072−4076.
(42) Bettinger, C.; Langer, R.; Borenstein, J. Engineering Substrate Topography at the Micro- and Nanoscale to Control Cell Function. *Angew. Chem., Int. Ed.* **2009**, *48*, 5406−5415.
(43) Lim, J. Y.; Donahue, H. J. Cell Sensing and Response to Micro- and Nanostructured Surfaces Produced by Chemical and Topographic Patterning. *Tissue Eng.* **2007**, *13*, 1879−1891.
(44) Martínez, E.; Lagunas, A.; Mills, C. A.; Rodríguez-Seguí, S.; Estévez, M.; Oberhansl, S.; Comelles, J.; Samitier, J. Stem Cell Differentiation by Functionalized micro- and nanostructured surfaces. *Nanomedicine* **2009**, *4*, 65−82.
(45) Pavlidis, P.; Noble, W. S. Matrix2png: A Utility for Visualizing Matrix Data. *Bioinformatics* **2003**, *19*, 295−296.
(46) Dahlstrand, J.; Zimmerman, L. B.; McKay, R. D.; Lendahl, U. Characterization of the Human Nestin Gene Reveals a Close Evolutionary Relationship to Neurofilaments. *J. Cell Sci.* **1992**, *103*, 589−597.
(47) Nichols, J. E.; Niles, J. A.; DeWitt, D.; Prough, D.; Parsley, M.; Vega, S.; Cantu, A.; Lee, E.; Cortiella, J. Neurogenic and Neuroprotective Potential of a Novel Subpopulation of Peripheral Blood-derived CD133+ ABCG2+CXCR4+ Mesenchymal Stem Cells: Development of Autologous Cell-based Therapeutics for Traumatic Brain Injury. *Stem Cell Res. Ther.* **2013**, *4*, 3.
(48) McCormick, M. B.; Tamimi, R. M.; Snider, L.; Asakura, A.; Bergstrom, D.; Tapscott, S. J. NeuroD2 and NeuroD3: Distinct Expression Patterns and Transcriptional Activation Potentials within the NeuroD Gene Family. *Mol. Cell. Biol.* **1996**, *16*, 5792−800.
(49) Dehmelt, L.; Halpain, S. Actin and Microtubules in Neurite Initiation: Are MAPs the Missing Link? *J. Neurobiol.* **2004**, *58*, 18−33.
(50) Roskams, A. J. I.; Cai, X.; Ronnett, G. V. Expression of Neuron-specific Beta-III Tubulin during Olfactory Neurogenesis in the Embryonic and Adult Rat. *Neuroscience* **1998**, *83*, 191−200.
(51) Mattila, P. K.; Lappalainen, P. Filopodia: Molecular Architecture and Cellular Functions. *Nat. Rev. Mol. Cell Biol.* **2008**, *9*, 446−454.
(52) Guillou, H.; Depraz-Depland, A.; Planus, E.; Vianay, B.; Chaussy, J.; Grichine, A.; Albigès-Rizo, C.; Block, M. R. Lamellipodia Nucleation by Filopodia Depends on Integrin Occupancy and Downstream Rac1 Signaling. *Exp. Cell Res.* **2008**, *314*, 478−488.
(53) Partridge, M. A.; Marcantonio, E. E. Initiation of Attachment and Generation of Mature Focal Adhesions by Integrin-containing Filopodia in Cell Spreading. *Mol. Biol. Cell* **2006**, *17*, 4237−4248.
(54) Hynes, R. O. Integrins: Bidirectional, Allosteric Signaling Machines. *Cell* **2002**, *110*, 673−687.
(55) Prowse, A. B. J.; Chong, F.; Gray, P. P.; Munro, T. P. Stem Cell Integrins: Implications for Ex-vivo Culture and Cellular Therapies. *Stem Cell Res.* **2011**, *6*, 1−12.
(56) Campos, L. S.; Leone, D. P.; Relvas, J. B.; Brakebusch, C.; Fässler, R.; Suter, U.; ffrench-Constant, C. β1 Integrins Activate a MAPK Signalling Pathway in Neural Stem Cells that Contributes to Their Maintenance. *Development* **2004**, *131*, 3433−3444.
(57) Rossier, O. M.; Gauthier, N.; Biais, N.; Vonnegut, W.; Fardin, M. A.; Avigan, P.; Heller, E. R.; Mathur, A.; Ghassemi, S.; Koeckert, M. S.; Hone, J. C.; Sheetz, M. P. Force Generated by Actomyosin Contraction Builds Bridges between Adhesive Contacts. *EMBO J.* **2010**, *29*, 1055−1068.
(58) Yu, H.; Lui, Y. S.; Xiong, S.; Leong, W. S.; Wen, F.; Nurkahfianto, H.; Rana, S.; Leong, D. T.; Ng, K. W.; Tan, L. P. Insights into the Role of Focal Adhesion Modulation in Myogenic Differentiation of Human Mesenchymal Stem Cells. *Stem Cells Dev.* **2013**, *22*, 136−147.
(59) Korobova, F.; Svitkina, T. Arp2/3 Complex Is Important for Filopodia Formation, Growth Cone Motility, and Neuritogenesis in Neuronal Cells. *Mol. Biol. Cell* **2008**, *19*, 1561−1574.

DOI: 10.1021/acsami.5b09588
ACS Appl. Mater. Interfaces 2016, 8, 563−573